Sussex Research Online

# Cosmological parameter estimation and the inflationary cosmology

Article (Published Version)

Leach, Samuel M, Liddle, Andrew R, Martin, Jérôme and Schwarz, Dominik J (2002) Cosmological parameter estimation and the inflationary cosmology. Physical Review D, 66 (2). 023515.

This version is available from Sussex Research Online: http://sro.sussex.ac.uk/id/eprint/23909/

This document is made available in accordance with publisher policies and may differ from the published version or from the version of record. If you wish to cite this item you are advised to consult the publisher's version. Please see the URL above for details on accessing the published version.

**Copyright and reuse:**
Sussex Research Online is a digital repository of the research output of the University.

Copyright and all moral rights to the version of the paper presented here belong to the individual author(s) and/or other copyright owners. To the extent reasonable and practicable, the material made available in SRO has been checked for eligibility before being made available.

Copies of full text items generally can be reproduced, displayed or performed and given to third parties in any format or medium for personal research or study, educational, or not-for-profit purposes without prior permission or charge, provided that the authors, title and full bibliographic details are credited, a hyperlink and/or URL is given for the original metadata page and the content is not changed in any way.

http://sro.sussex.ac.uk

# Cosmological parameter estimation and the inflationary cosmology

Samuel M. Leach,[1,*] Andrew R. Liddle,[1,†] Jérôme Martin,[2,‡] and Dominik J. Schwarz[3,§]
[1]*Astronomy Centre, University of Sussex, Brighton BN1 9QJ, United Kingdom*
[2]*Institut d'Astrophysique de Paris, 98bis boulevard Arago, 75014 Paris, France*
[3]*Institut für Theoretische Physik, Technische Universität Wien, Wiedner Hauptstraße 8-10, 1040 Wien, Austria*
(Received 6 February 2002; published 18 July 2002)

We consider approaches to cosmological parameter estimation in the inflationary cosmology, focusing on the required accuracy of the initial power spectra. Parametrizing the spectra, for example by power laws, is well suited to testing the inflationary paradigm but will only correctly estimate cosmological parameters if the parametrization is sufficiently accurate, and we investigate conditions under which this is achieved both for present data and for upcoming satellite data. If inflation is favored, reliable estimation of its physical parameters requires an alternative approach adopting its detailed predictions. For slow-roll inflation, we investigate the accuracy of the predicted spectra at first and second order in the slow-roll expansion (presenting the complete second-order corrections for the tensors for the first time). We find that, within the presently allowed parameter space, there are regions where it will be necessary to include second-order corrections to reach the accuracy requirements of MAP and Planck satellite data. We end by proposing a data analysis pipeline appropriate for testing inflation and for a cosmological parameter estimation from high-precision data.

DOI: 10.1103/PhysRevD.66.023515 PACS number(s): 98.80.Cq, 98.70.Vc

## I. INTRODUCTION

Recent cosmic microwave background (CMB) anisotropy results [1], showing a multiple peak structure in the anisotropy power spectrum, lend powerful support to the inflationary cosmology as the origin of structure in the Universe. It is now widely expected that cumulative improvements in the CMB data will lead to a progressively more accurate estimation of cosmological parameters, with projects funded so far culminating in the Planck satellite mission expected to report results around 2010.

Given a set of data on structures in the Universe, such as the CMB power spectrum, it is necessary to simultaneously fit both for the parameters describing the global cosmology (such as the matter budget and expansion rate) and those describing the so-called ''initial perturbations''; they cannot be considered separately. If the model for the initial perturbations is insufficiently accurate, or even worse completely wrong, the full power of the experiment to constrain cosmological parameters cannot be exploited.

The inflationary cosmology is an attractive paradigm for the generation of the initial perturbations, but even there the situation can be very complicated in general. In particular, if there are multiple scalar fields the perturbations can be a mixture of isocurvature and adiabatic, and may be non-Gaussian. Such initial conditions may prove difficult or even impossible to parametrize, and if such an inflation model is correct it will be a major obstacle to successful parameter estimation. However it remains a powerful working hypothesis that the simplest class of models, where inflation is driven by a single scalar field, is viable; this creates a framework within which the necessary calculations are reasonably simple, with the initial perturbations computed either approximately analytically or exactly numerically. As yet, there is no indication from observations that we might need to go beyond this paradigm.

The main goal of this article is to investigate different strategies that an observer can use to estimate the cosmological parameters, and to examine the extent to which it is necessary to adopt detailed inflationary predictions. The spectrum of the fluctuations is assumed to be produced by an underlying inflationary model and is calculated exactly by means of numerical computations. Given this situation, we study how the data analysis can be performed in two different scenarios. The first scenario applies if one wants only to estimate cosmological parameters, such as the baryon density and reionization optical depth, and does not care about the underlying inflation model beyond being confident that the description of the initial perturbations used is adequate. In this case, observers typically use a power-law fit, see e.g. Ref. [1], and the first question is to test how accurate a power-law fit is to typical inflationary cosmologies. In particular, we wish to know if this kind of fit is accurate enough for present data, and whether it will also be accurate enough to analyze high-precision data like that to be provided by the Planck satellite. The second scenario, which makes more stringent requirements on theoretical accuracy, is if one intends to estimate properties of the inflationary model. In this case, the slow-roll method can be used to calculate an approximate spectrum and we will study its accuracy. We also consider to which order in the slow-roll parameters the spectrum should be calculated in order to reach the Planck precision. We propose an analysis pipeline for testing the consistency of single-field slow-roll inflation and estimating physical parameters of inflation, e.g. the energy scale of inflation.

*Electronic address: s.m.leach@sussex.ac.uk
†Electronic address: a.liddle@sussex.ac.uk
‡Electronic address: jmartin@iap.fr
§Electronic address: dschwarz@hep.itp.tuwien.ac.at

 ©2002 The American Physical Society

## II. INFLATIONARY BASICS

A single-field inflation model generates Gaussian spectra of purely adiabatic density perturbations (scalar perturbations) and gravitational waves (tensor perturbations). We denote the dimensionless power spectra by $\mathcal{P}_{\mathcal{R}}(k)$, where $\mathcal{R}$ is the intrinsic curvature perturbation on comoving hypersurfaces (identical with Bardeen's $\zeta$ [2] up to a sign), and $\mathcal{P}_h(k)$, $h$ being the amplitude of gravitational waves. Scalar and tensor perturbations obey the equation of a parametric oscillator [3]

$$\mu''_{\mathrm{S,T}} + \left( k^2 - \frac{z''_{\mathrm{S,T}}}{z_{\mathrm{S,T}}} \right) \mu_{\mathrm{S,T}} = 0, \tag{1}$$

where a prime denotes differentiation with respect to conformal time $\eta$ and $k$ is the comoving wavenumber. This equation only requires the assumption of linear perturbation theory. The quantities $\mu_{\mathrm{S,T}}(\eta)$ are defined by $\mu_{\mathrm{S}}(\eta) \equiv 2 z_{\mathrm{S}} \mathcal{R}$ and $\mu_{\mathrm{T}}(\eta) \equiv z_{\mathrm{T}} h$ where $z_{\mathrm{S}} \equiv a\sqrt{-aa''}/a'$ and $z_{\mathrm{T}} = a$. The initial conditions for the mode functions $\mu_{\mathrm{S,T}}$ are fixed by the assumption that the quantum fields are in the vacuum state when the mode $k$ is subhorizon,

$$\lim_{k/aH \to \infty} \mu_{\mathrm{S,T}}(\eta) = \frac{4\sqrt{\pi}}{m_{\mathrm{Pl}}} \frac{e^{-ik(\eta - \eta_{\mathrm{i}})}}{\sqrt{2k}}, \tag{2}$$

where $\eta_{\mathrm{i}}$ is an arbitrary initial time at the beginning of inflation. The power spectra are calculated according to

$$\mathcal{P}_{\mathcal{R}}(k) = \frac{k^3}{8\pi^2} \left| \frac{\mu_{\mathrm{S}}}{z_{\mathrm{S}}} \right|^2, \quad \mathcal{P}_h(k) = \frac{2k^3}{\pi^2} \left| \frac{\mu_{\mathrm{T}}}{z_{\mathrm{T}}} \right|^2. \tag{3}$$

Both power spectra can be derived from the inflaton potential $V(\phi)$ and the initial conditions for the inflaton field $\phi$, and hence are not independent. They can be obtained numerically by solving the appropriate mode equations wave number by wave number (see e.g. Ref. [4]). In the following, they are denoted by $\mathcal{P}_{\mathrm{num}}(k)$.

The tensor-to-scalar ratio

$$R \equiv \frac{\mathcal{P}_h}{\mathcal{P}_{\mathcal{R}}}, \tag{4}$$

is of interest for testing the consistency of a given model of inflation. It has often been defined in terms of the microwave background quadrupole moments. This definition has the disadvantage that it depends on the cosmological parameters, especially the density of the cosmological constant $\Omega_\Lambda$ [5,6]. In Ref. [7] the ratio between $\mathcal{P}_\Phi$ (where $\Phi$ is the gauge-invariant Bardeen metric potential [8]) and $\mathcal{P}_h$ was used, which removes the dependence on $\Omega_\Lambda$. However $\Phi$ does still depend on the dynamics of the Universe at the photon decoupling epoch and thus is not completely model independent (it depends mainly on the physical matter density $\omega_{\mathrm{m}} \equiv \Omega_{\mathrm{m}} h^2$). The advantage of $\mathcal{R}$ is that it is conserved on super-horizon scales once the decaying mode is negligible and provided only adiabatic perturbations are considered [2,9,10].

The spectral indices and their "running" are defined by the following expressions:

$$n_{\mathrm{S}}(k) - 1 \equiv \frac{d \ln \mathcal{P}_{\mathcal{R}}}{d \ln k}, \quad n_{\mathrm{T}}(k) \equiv \frac{d \ln \mathcal{P}_h}{d \ln k}, \tag{5}$$

$$\alpha_{\mathrm{S}}(k) \equiv \frac{dn_{\mathrm{S}}}{d \ln k}, \quad \alpha_{\mathrm{T}}(k) \equiv \frac{dn_{\mathrm{T}}}{d \ln k}. \tag{6}$$

For purposes of illustration, in this paper we use three qualitatively different inflationary models to mimic idealized measurements of the power spectra. The first is a chaotic inflation model with a quartic potential [11]

$$V(\phi) = \lambda \phi^4, \tag{7}$$

the second a false vacuum inflation potential

$$V(\phi) = V_0 \left[ 1 + \frac{1}{2} \mu^2 \left( \frac{\phi}{m_{\mathrm{Pl}}} \right)^2 \right], \tag{8}$$

with $\mu^2 = 1$, which is inspired by the scenario of hybrid inflation [12], and the third a potential introduced in Ref. [13]:

$$V(\phi) = V_0 \left[ 1 - \frac{2}{\pi} \arctan\left( 5 \frac{\phi}{m_{\mathrm{Pl}}} \right) \right]. \tag{9}$$

For each potential we need to know the scalar field value $\phi_*$ when observable perturbations were generated (i.e. when a given scale $k_*$ was equal to the Hubble radius during inflation), corresponding roughly to 55 $e$-foldings from the end of inflation. The last two potentials provide no natural end to inflation, and we make an arbitrary choice for $\phi_*$ to be equal $0.3\sqrt{2} m_{\mathrm{Pl}}$ and $-0.3 m_{\mathrm{Pl}}$ respectively. The chaotic inflation model ends by violation of slow roll and so we take $\phi_* \simeq 4.2 m_{\mathrm{Pl}}$.

Figure 1 shows the scalar and tensor power spectra $\mathcal{P}_{\mathrm{num}}(k)$ for these three models, obtained numerically by the method of Ref. [4]. The corresponding microwave anisotropies, obtained using a modified version of CAMB [14], are also shown.[1] We present the characteristic quantities of these spectra, evaluated at $k_*$, in Table I. We have chosen these three models because the chaotic model is an example in which tensor perturbations are relevant and it shows moderate negative tilt, the false vacuum model has a moderate positive tilt and the arctan model has both large tilt and running.

## III. PARAMETER ESTIMATION IGNORING INFLATIONARY PREDICTIONS

### A. Parametrizing the spectra

To estimate the cosmological parameters we need an adequate parametrization of scalar perturbations, and more sophisticated analyses informed by inflation also include

[1] A module to directly input the predictions of slow-roll inflation to the CAMB program is available to download at www.astronomy.susx.ac.uk/~sleach/inflation/

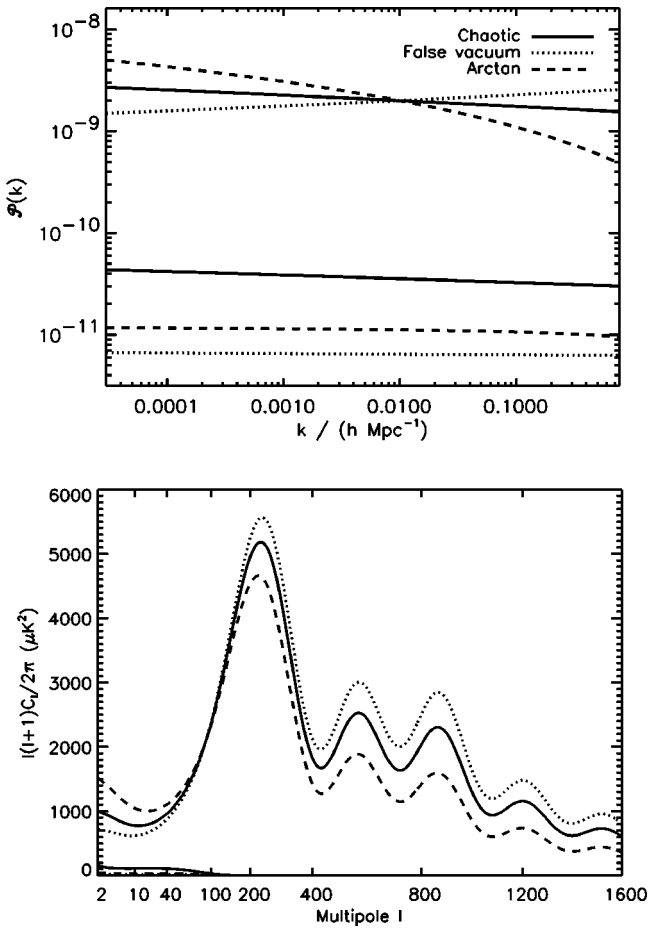


FIG. 1. The top panel shows the power spectra of scalar (upper lines) and tensor (lower lines) perturbations for our three models. The scalar spectra are normalized to $\mathcal{P}_{\mathcal{R}}=2\times10^{-9}$ at the scale $k_*=0.01h$ Mpc$^{-1}$, which approximately matches the Cosmic Background Explorer (COBE) normalization. The bottom panel shows the corresponding $C_l$ curves for a flat cosmological model with $\omega_b=0.0200$, $\omega_m=0.1268$ and $\omega_\Lambda=0.2958$ (implying $h=0.65$), and reionization optical depth $\tau=0.05$, with the upper lines again the scalar contribution and the tensors considerably subdominant. Only the sum of the two can be detected, though they contribute differently to polarization anisotropies.

tensors.[2] If one is only interested in a measurement of those cosmological parameters that do not describe the initial perturbations, one would like to know whether robust results can be obtained using simple forms for the initial power spectra rather than detailed inflationary predictions. Therefore, in the context envisaged in this section, the observer does not use the assumption that inflation is the correct underlying theory, other than to motivate the restriction of the scalar perturbations to be adiabatic.

It is common practice to assume a power-law shape for the spectrum specified by an amplitude and a spectral index. The reasoning for this parametrization is its simplicity. In the absence of any physical model for the generation of fluctuations, one assumes that there is no distinguished physical scale in the primordial power spectra. In order to allow for mildly scale-dependent power spectra, a running of the spectral indices can be included. This leads to the following shape:

$$\mathcal{P}_{\rm fit}(k)=\mathcal{P}_{\rm fit}(k_*)\left(\frac{k}{k_*}\right)^{n_{\rm fit}+(1/2)\alpha_{\rm fit}\ln(k/k_*)}, \qquad (10)$$

where $n_{\rm fit}$ is either $n_S-1$ or $n_T$.[3] The pivot scale $k_*$ is the scale at which all the quantities are evaluated. A useful way of viewing Eq. (10) is that it is the first terms of a Taylor expansion of $\ln\mathcal{P}(k)$ in $\ln k$ about the pivot scale, which draws one's attention to the possibility of using other expansions.

TABLE I. Numerical values of spectral indices, their running and the tensor-to-scalar ratio for the three models considered. All quantities are evaluated at $k_*=0.01h$ Mpc$^{-1}$.

| Exact values | $R$ | $n_S-1$ | $n_T$ | $\alpha_S$ | $\alpha_T$ |
|---|---|---|---|---|---|
| Chaotic | 0.285 | −0.055 | −0.037 | −0.0009 | −0.0006 |
| False vacuum | 0.051 | 0.054 | −0.006 | 0.0018 | 0.0005 |
| Arctan model | 0.089 | −0.216 | −0.015 | −0.0298 | −0.0036 |

The simplest assumption would be to take both spectra as constant (scale-invariant). Models with $n_S-1=0$ and $n_T=0$ do in fact provide acceptable fits to recent CMB data (for sufficiently low or zero tensor amplitude); thus, if we decide to ignore inflation for the moment, there is no reason from CMB observations alone to include a tilt. Reference [7] quotes $n_S-1=-0.07^{+0.75}_{-0.16}$ at 95% confidence level, and the addition of large-scale structure data greatly tightens the constraint without altering the conclusion that $n_S=1$ is allowed. Current observational constraints on the running of the spectral index are far weaker than the magnitude predicted in popular inflationary models. Thus far, only upper limits on the contribution of gravitational waves have been derived [7,15,16]. Some of these limits suffer from the problems described below Eq. (4), and use strong priors on some of the other cosmological parameters. Translating the result of Fig. 5 of Ref. [7] ($r<0.5$ at 95% confidence level) to our notation gives $R=9r/25<0.2$, while Ref. [16] gives a weaker constraint also consistent with $R=0$. Let us also remark that the majority of recent papers estimating parameters from the microwave background have done so under the assumption that the scalar spectrum has a power-law shape and that there is no contribution from tensor perturbations ($R=0$).

The question of how far power spectra expansions should be taken, and how accurately their coefficients need to be computed, obviously depends on the accuracy and dynamic range of observations. For present observations an accuracy level of ten percent or better is certainly required. Ultimately,

[2]A general analysis would also have to consider vector modes and the various possible isocurvature modes, but at present there is no evidence that they are required.

[3]Note from the definition of the spectral index that $n_S(k)-1\neq n_{\rm fit}+\frac{1}{2}\alpha_{\rm fit}\ln(k/k_*)$ away from the pivot scale.

Planck will measure multipole moments $C_l$ from $l$ of 2 to about 2000, corresponding to $\Delta \ln k/k_* \simeq 3.5$ on either side of a central pivot $k_*$. It is rather unclear how accurately the multipole moments need to be represented at the extremes (cosmic variance intervening on large scales and the damping tail removing the signal on short scales), but in the center an accuracy of better than one percent is certainly desired (see e.g., Ref. [17]).[4] If one then further assumes that Planck data will be combined with high-accuracy galaxy correlation data, the $k$ range might extend to around $\Delta \ln k/k_* \simeq 6$ (corresponding to $k_{\max} \simeq 30h$ Mpc$^{-1}$), though the nonlinearly evolved galaxy power spectrum on short scales is unlikely to be amenable to extremely accurate multiparameter estimation. The choice of pivot scale $k_*$ is important as the difference between the fitted and the true power spectrum produces an error that runs as we move away from the pivot scale. While a careful tracking of error covariances should lead to results independent of the choice of pivot, those covariances should be minimized to a good approximation by aligning $k_*$ with $l_*$, the multipole where we expect the observational errors to be least. One can use the approximation [19]

$$k_* = \frac{H_0}{2} \frac{\sqrt{\Omega_{\rm m}}}{1 + 0.084 \ln \Omega_{\rm m}} l_*, \quad \Omega_{\rm m} + \Omega_\Lambda = 1, \tag{11}$$

where $H_0 = h/3000$ Mpc$^{-1}$ to carry out this alignment.

Having described the typical errors in the multipole moments, Error($C_l$), we now need to link this quantity to the error in the power spectrum itself, Error($\mathcal{P}$), since this is the quantity calculated in practice. We assume throughout this paper that an error in our determination of the power spectrum propagates directly to an error in our determination of the $C_l$'s since

$$C_l = 4\pi \int d \ln k \mathcal{P}(k) [\Delta_l(k)]^2, \tag{12}$$

where $\Delta_l(k)$ is the $l$-th momentum of the temperature fluctuations. In other words, we assume Error($C_l$) $\simeq$ Error($\mathcal{P}$).

Another question is how an error in the power spectrum propagates to an error in the estimation of the cosmological parameters. In general the Fisher matrix formulation is needed to estimate how well a given experiment can measure the parameters; the error in the cosmological parameters is not simply related to the error in the power spectrum as there are many parameters and lots of degeneracies amongst them. The requirement Error($\mathcal{P}$) $\simeq 1\%$ for Planck is a very stringent condition. In particular, it does not imply that parameter estimates would go astray if we drifted outside our power spectrum accuracy criterion; we would expect parameter estimates to stabilize some way before the fitted power spectrum was within our 1% accuracy everywhere. Our criterion is a sufficient and conservative condition for establishing a safe procedure: as long as the power spectrum accuracy is below 1% everywhere, we are confident that the systematic errors coming from an inaccurate parametrization of the initial conditions will not play a role in the data analysis of an experiment like Planck.

[4]We note that current implementations of CMBFAST [18] and CAMB [14] have a target accuracy of one percent, so there is presently nothing to gain by demanding power spectrum accuracy much higher than this.

### B. Accuracy of the parametrized spectra

We now investigate the systematic errors which might arise from assuming that the spectra have perfect power-law shapes or, in a more sophisticated version, a constant value for the running of the spectral index. The first step is to fix the numerical values of the coefficients $\mathcal{P}_{\rm fit}(k_*)$, $n_{\rm fit}$ and $\alpha_{\rm fit}$. We have no means to calculate them theoretically in the present context. In practice, observers determine these coefficients by carrying out a fit to the data. Here, we carry out a least-squares fit of $\mathcal{P}_{\rm fit}(k)$ to $\mathcal{P}_{\rm num}(k)$ to obtain best-fit scale-invariant, power-law and power-law plus running spectra. This means that the coefficients $\mathcal{P}_{\rm fit}(k_*)$, $n_{\rm fit}$ and $\alpha_{\rm fit}$ are those for which the quantity

$$\sum_i [\mathcal{P}_{\rm fit}(k_i) - \mathcal{P}_{\rm num}(k_i)]^2 \tag{13}$$

is minimized. We took the $k_i$ to be equally spaced in $d \ln k$ and given equal weight. This idealized fitting approach will tend to sacrifice accuracy in the center of desired range in favor of accuracy at the extremes. Here the idea is to test whether in principle the shape of $P_{\rm fit}$ can reproduce the true power spectrum over a reasonable range in $k$. This obviously becomes important if, for example, we try to use a power-law shape to fit to a model with significant running of the spectral index. The result of the minimization procedure for the three models introduced above is summarized in Table II. These values should be compared with the exact ones of Table I.

For the first two examples we conclude that the sequence of fitting a constant amplitude, a power-law, and finally a power-law with running provides best-fit values which reproduce the numerical values with sufficient accuracy. From the observational point of view this is reflected in the fact that the best-fit value of $R$ is the same in the second and third row and that the fit values of the spectral indices are almost the same as well. Such a behavior is the experimental evidence that the input does make sense. The situation is different for our third example, the arctan model. Although there is slow convergence in the best-fit values of $R$, no sign of convergence can be detected by inspection of Table II in the spectral indices. This is confirmed by a comparison with the numerical values of Table I, e.g., the fitted spectral index of the tensors is less precise in the third row than in the second, the scalar spectral index is underestimated by 0.036 by the power-law fit and overestimated by 0.022 including running. From the point of view of inflationary parameters, see below, these are large fluctuations. Thus an observer in possession of sufficiently accurate data sometime in the future should conclude for our third example that more parameters have to

TABLE II. The ratio of the fitted amplitude to the numerical amplitude of the scalars, $A_{\rm fit/num}$, and the best-fit values of the tensor-to-scalar ratio, the spectral indices and their running for the three models considered at $k_*=0.01h$ Mpc$^{-1}$. For each model, we present the results for a scale-invariant, power-law and power-law with running spectral shape in three rows respectively.

| Fitted values | $A_{\rm fit/num}$ | $R$ | $n_{\rm S}-1$ | $n_{\rm T}$ | $\alpha_{\rm S}$ | $\alpha_{\rm T}$ |
|---|---|---|---|---|---|---|
| Chaotic | 1.05 | 0.279 | | | | |
| | 1.00 | 0.285 | −0.054 | −0.036 | | |
| | 1.00 | 0.285 | −0.055 | −0.037 | −0.0010 | −0.0007 |
| False vacuum | 0.98 | 0.053 | | | | |
| | 1.01 | 0.051 | 0.054 | −0.006 | | |
| | 1.00 | 0.051 | 0.054 | −0.006 | 0.0017 | 0.0004 |
| Arctan model | 1.23 | 0.072 | | | | |
| | 0.95 | 0.092 | −0.178 | −0.016 | | |
| | 0.99 | 0.090 | −0.238 | −0.020 | −0.0303 | −0.0044 |

be introduced in the fit, before any physical meaning can be extracted from the best-fit values of the spectral indices.

A large error in the fitted values of the amplitude and of the spectral index, even if we are not interested in the physics of inflation for the moment, is undesirable for two reasons. First the overall amplitude of scalar perturbations is a quantity that we hope to measure from Microwave Anisotropy Probe (MAP) and Planck at the percent level. Thus we would prefer to relate it to a physical quantity, namely the amplitude of superhorizon density fluctuations. The second reason comes from considerations of large-scale structure data, where it is customary to include a linear bias parameter, $b$, to account for the overall normalization of the matter power spectrum. If we simultaneously fit to the CMB, then we can only assign any physical meaning to $b$ if we are certain that the amplitude of scalar perturbations is correct. In addition, an inaccurate estimate of the amplitude and the tilt could spoil a consistency check of structure formation based on measurements of $\sigma_8$.

Having determined the coefficients, the second step is now to compute the error. We define this by

$$\mathrm{Error}(\mathcal{P})\equiv\left(\frac{\mathcal{P}_{\rm fit}}{\mathcal{P}_{\rm num}}-1\right)\times 100\%. \tag{14}$$

In the following, we give three examples.

In Fig. 2 we plot the error in the scalar power spectrum in the case of the false vacuum model. The best-fit scale-invariant spectrum is a poor fit for this particular model, while the best-fit power-law spectrum improves things greatly, keeping the errors below 2% which is more than adequate for present CMB data and marginally adequate for Planck. The large effect of the tilt is due to a long lever arm in wavenumbers [20]; the error being of the order $(n_{\rm S}-1)\ln k/k_*$, even a small tilt can have a significant effect if the data span several decades in wavenumbers. We can further see that with the inclusion of running, $P_{\rm fit}$ now reproduces the power spectrum in great detail. This is because the correction to the spectrum is of order $\alpha_{\rm S}\ln^2 k/k_*$ which, for the running of this example of $\alpha_{\rm S}\simeq 0.002$, gives a significant effect though the correction is much smaller than that from the tilt.

Given a set of observations, the importance of running is tested by including it in the fit and examining whether the fit improves significantly. In the absence of any theoretical prejudice, one might well hope to detect significant running at high significance. However, some of the simplest inflation models predict running of at least an order of magnitude below what even Planck can achieve [21]. In that case there will be no significant detection of running, and marginalizing over the running permitted by the observations may lead to a significant inflating of errors on other parameters. While combining short-scale observations with the microwave background may give a stronger lever-arm in constraining running, this may well turn out to be a parameter for which it is desirable to investigate imposing a strict theoretically-motivated prior to compare with a free fit. Further, even if running is detected at high significance this problem then resurfaces concerning the running of running.

As we have already concluded from the discussion of the best-fit values in Table II, there exist models for which a power-law fit to the spectrum does not provide a good de-

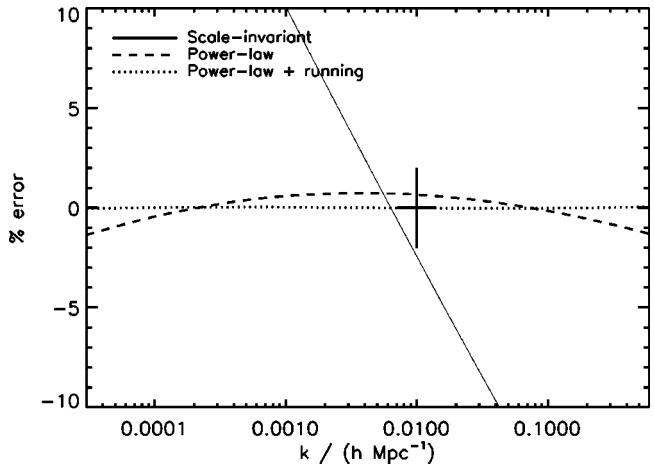


FIG. 2. Error curves for various fits to the scalar power spectrum for the false vacuum model. While the power-law fit is acceptable for fitting to present data, neglecting running affects the estimate of the power spectrum amplitude at the pivot point at the percent level.

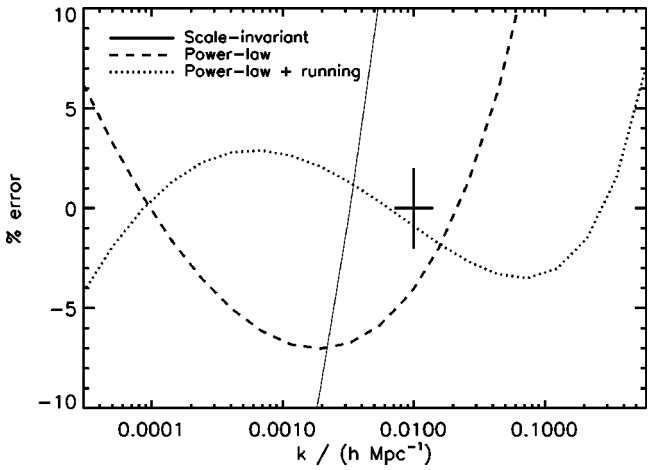


FIG. 3. As Fig. 2 but for the arctan model. For fitting to data of the present quality, the inclusion of the running is required.

scription in contrast to the above example. In Fig. 3 the error in the scalar power spectrum for the arctan model is displayed. Including the running is necessary for the present accuracy of CMB experiments. Now the effect of running is comparable to that of the tilt. We see that more parameters (e.g. running of the running) would be necessary to reproduce the power spectrum with 1% accuracy. We actually have to add more and more parameters until the spectrum starts to converge (see also the discussion of Table II), or consider using a different spectral shape.

For the tensors in the case of the chaotic model, we see in Fig. 4 that the spectrum is poorly fitted by the scale-invariant spectrum. However, the accuracy requirements on the tensor spectrum are less stringent—the tensor amplitude is generally less than the scalar amplitude and so the required absolute error in $\mathcal{P}_{\rm h}$ is also less $[\simeq R\times\mathrm{Error}(\mathcal{P}_{\mathcal{R}})]$. Thus, a typical inflationary tensor spectrum is well described even by a scale-invariant spectrum for present-day experiments, though there is no reason not to describe it with the same sophistication as the scalar spectrum. For future CMB measurements, the inclusion of a tilt is sufficient in this example.

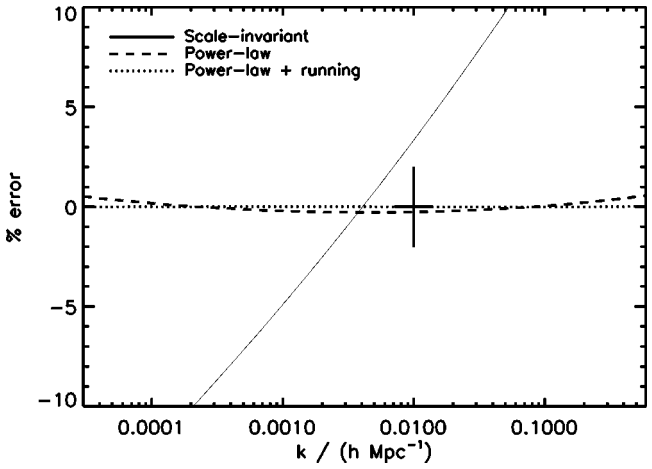


FIG. 4. As Fig. 2 but for the chaotic inflation model tensor spectrum. Although the percentage error is large for the scale-invariant fit, the absolute error is small compared to the scalar spectrum, and so the scale-invariant fit is still acceptable.

To answer the main question of this section, we can expect to obtain robust estimates for the cosmological parameters for a restricted class of inflationary models using the fitting procedure described above. However, there exist models where this is no longer true. In the following sections, we specify the criteria which define this class of models.

## IV. PREDICTIONS OF SLOW-ROLL INFLATION

In this section, we restrict our considerations to the class of slow-roll models of inflation. The advantage is that we can now predict the shape of the power spectra and link the parameters characterizing these spectra to the physics of inflation. There has recently been renewed progress in the accurate calculation of inflationary perturbations by analytical techniques, including a computation of the power spectra to arbitrary order in the slow-roll expansion for single-field inflation by Stewart and Gong [22], and a computation at higher order for models that may violate one of the slow-roll conditions [23,24]. We utilize the Stewart-Gong results here as they have the most general applicability, extending them with an explicit evaluation of higher-order terms for the tensor spectrum.

The background evolution can be described in terms of the horizon-flow parameters $\{\epsilon_n\}$ [24]. Starting from $\epsilon_0\equiv H(N_{\rm i})/H(N)$, where $1/H$ is the Hubble distance and $N\equiv\ln(a/a_{\rm i})$ the number of $e$-folds since some initial time $t_{\rm i}$, the set $\{\epsilon_n\}$ is defined by

$$\epsilon_{n+1}\equiv\frac{d\ln|\epsilon_n|}{dN},\quad n\geqslant 0. \tag{15}$$

These parameters can be easily related to various definitions of the slow-roll parameters. Setting $n=1$ we find $\epsilon_1=-d\ln H/d\ln a$, which is nothing but the slow-roll parameter $\epsilon$ of Refs. [25,26]. The parameter $\eta$ of Refs. [25,26], which is usually defined to measure the deceleration of the inflaton field, enters as $\epsilon_2=2\epsilon-2\eta$. The third slow-roll parameter, $\xi$, is contained in $\epsilon_2\epsilon_3=4\epsilon^2-6\epsilon\eta+2\xi^2$. In this notation, all the $\epsilon_n$ are typically of the same order of magnitude. Inflation takes place provided $\epsilon_1<1$. Slow-roll inflation is defined by the condition $|\epsilon_n|\ll 1$, for all $n>0$.

A measurement of the horizon-flow parameters, at a specific moment during inflation, would immediately provide us with a value for the inflaton potential $V$ and its derivatives with respect to the inflaton field $\phi$ (denoted by a prime in what follows) for any single-field inflation model. For example, from $H$ and $\epsilon_1,\epsilon_2$, and $\epsilon_3$ we can calculate the potential and its first two derivatives exactly,

$$V=\frac{3m_{\rm Pl}^2H^2}{8\pi}\left(1-\frac{\epsilon_1}{3}\right), \tag{16}$$

$$V'=-\frac{3m_{\rm Pl}H^2}{(4\pi)^{1/2}}\epsilon_1^{1/2}\left(1-\frac{\epsilon_1}{3}+\frac{\epsilon_2}{6}\right), \tag{17}$$

$$\frac{V''}{3H^2}=2\epsilon_1-\frac{\epsilon_2}{2}-\frac{2\epsilon_1^2}{3}+\frac{5\epsilon_1\epsilon_2}{6}-\frac{\epsilon_2^2}{12}-\frac{\epsilon_2\epsilon_3}{6}. \tag{18}$$

If $\epsilon_3$ cannot be determined and the horizon-flow parameters are small compared to unity, we can still estimate $V''$ by keeping the leading terms only.

For slow-roll models we can invert this procedure and estimate the horizon-flow parameters. At leading order in these parameters we find

$$H^2\simeq\frac{8\pi}{3m_{\rm Pl}^2}V, \tag{19}$$

$$\epsilon_1\simeq\frac{m_{\rm Pl}^2}{16\pi}\left(\frac{V'}{V}\right)^2, \tag{20}$$

$$\epsilon_2\simeq\frac{m_{\rm Pl}^2}{4\pi}\left[\left(\frac{V'}{V}\right)^2-\frac{V''}{V}\right], \tag{21}$$

$$\epsilon_2\epsilon_3\simeq\frac{m_{\rm Pl}^4}{32\pi^2}\left[\frac{V'''V'}{V^2}-3\frac{V''}{V}\left(\frac{V'}{V}\right)^2+2\left(\frac{V'}{V}\right)^4\right]. \tag{22}$$

To give an example, for chaotic inflation with the potential $V\propto\phi^\gamma$ we find $\epsilon_1\simeq\gamma/4\Delta N$ and $\epsilon_2\simeq\epsilon_3\simeq1/\Delta N$, where $\Delta N$ denotes the number of *e*-folds before inflation ends. Chaotic inflation is a simple model where the higher horizon-flow parameters are of the same order of magnitude as lower ones. In the case of power-law inflation ($a\propto t^p$) where the potential is given by $V\propto\exp[-(16\pi/p)^{1/2}\phi/m_{\rm Pl}]$, we recover the exact result $\epsilon_1=1/p$ and $\epsilon_2=\epsilon_3=0$.

The power spectra of scalar and tensor perturbations can be obtained approximately using analytic techniques. One expands the power spectra about some particular wave number $k_*$, and then computes the coefficients using the slow-roll expansion or some other scheme of approximation. This amounts to a double approximation. Given that we need to cover several orders of magnitude in $k$, the most appropriate expansion variable is $\ln k$, giving

$$\frac{\mathcal{P}(k)}{\mathcal{P}_0(k_*)}=a_0+a_1\ln\left(\frac{k}{k_*}\right)+\frac{a_2}{2}\ln^2\left(\frac{k}{k_*}\right)+\cdots. \tag{23}$$

The next step is to establish an expression for the coefficients $a_n$, which can be obtained either with help of the slow-roll expansion [6,20,22,25,27,28] or the methods of approximation developed in Refs. [23,24]. Since the former covers a more general class of inflation models than the latter, we focus on slow-roll inflation in the following. We will use the term *first order* to refer to results including all terms up to order $\epsilon_m$ and *second order* if one goes to terms including $\epsilon_m^2$.

The normalization of the power spectra is set by the expansion rate during inflation, $H$, and the parameter $\epsilon_1$: namely,

$$\mathcal{P}_{\mathcal{R}0}(k_*)=\frac{H^2}{\pi\epsilon_1 m_{\rm Pl}^2}, \tag{24}$$

$$\mathcal{P}_{h0}(k_*)=\frac{16H^2}{\pi m_{\rm Pl}^2}, \tag{25}$$

where $H$ and $\epsilon_1$ are evaluated when $aH=k_*$ during inflation. The scalar amplitude has been calculated up to first order in the slow-roll parameters by Stewart and Lyth [27], and recently up to second order by Stewart and Gong [22]. These calculations are sufficient to allow calculation of an infinite, though incomplete, set of expansion coefficients of which the first few are given by

$$\begin{aligned}a_{\rm S0}=&1-2(C+1)\epsilon_1-C\epsilon_2+\left(2C^2+2C+\frac{\pi^2}{2}-5\right)\epsilon_1^2\\&+\left(C^2-C+\frac{7\pi^2}{12}-7\right)\epsilon_1\epsilon_2+\left(\frac{1}{2}C^2+\frac{\pi^2}{8}-1\right)\epsilon_2^2\\&+\left(-\frac{1}{2}C^2+\frac{\pi^2}{24}\right)\epsilon_2\epsilon_3,\end{aligned} \tag{26}$$

$$\begin{aligned}a_{\rm S1}=&-2\epsilon_1-\epsilon_2+2(2C+1)\epsilon_1^2+(2C-1)\epsilon_1\epsilon_2+C\epsilon_2^2\\&-C\epsilon_2\epsilon_3,\end{aligned} \tag{27}$$

$$a_{\rm S2}=4\epsilon_1^2+2\epsilon_1\epsilon_2+\epsilon_2^2-\epsilon_2\epsilon_3, \tag{28}$$

where $C\equiv\gamma_{\rm E}+\ln2-2\approx-0.7296$. For the tensors, the corresponding set is as follows:

$$\begin{aligned}a_{\rm T0}=&1-2(C+1)\epsilon_1+\left(2C^2+2C+\frac{\pi^2}{2}-5\right)\epsilon_1^2\\&+\left(-C^2-2C+\frac{\pi^2}{12}-2\right)\epsilon_1\epsilon_2,\end{aligned} \tag{29}$$

$$a_{\rm T1}=-2\epsilon_1+2(2C+1)\epsilon_1^2-2(C+1)\epsilon_1\epsilon_2, \tag{30}$$

$$a_{\rm T2}=4\epsilon_1^2-2\epsilon_1\epsilon_2. \tag{31}$$

We have presented for the first time the $\mathcal{O}(\epsilon_n^2)$ terms in the tensor amplitude which we obtained along the lines of Ref. [22].

The coefficients $a_n$ for $n>0$ can also be obtained by successive differentiation of the first term of the expansion

$$a_n\equiv\left.\frac{d^n[\mathcal{P}(k)/\mathcal{P}_0(k_*)]}{d\ln^n k}\right|_{k=k_*} \tag{32}$$

$$=\frac{1}{\mathcal{P}_0(k_*)}\left(\frac{1}{1-\epsilon_1}\frac{d}{dN}\right)^n\mathcal{P}_0(k_*)a_0(k_*), \tag{33}$$

where we used the "horizon crossing" condition $k_*=k=aH$ to obtain the second line. From Eqs. (15) and (32) we see that the leading contribution to $a_n$ is of order $\epsilon_m^n$ (where $\epsilon_m^n$ means any terms containing $n$ of the $\epsilon$, not necessarily all the same). If $a_0$ has been written to first order, differentiation yields $a_1$ to second order, $a_2$ to third order and so on. Note

that the coefficients of the Taylor series, Eq. (23), always feature an increasing number of powers of the slow-roll parameters, so in practice convergence of the Taylor series is governed by the size of $\epsilon_m \ln k/k_*$, which in principle needs to be small for all values of $m \geqslant 1$. Thus the series can still be strongly convergent even if $\ln k/k_*$ exceeds one, as it will for typical upcoming experiments.

Let us now calculate the spectral indices and their running in the slow-roll approximation up to second order. For this purpose, it is useful to calculate the logarithm of the power spectrum

$$\ln \frac{\mathcal{P}(k)}{\mathcal{P}_0(k_*)} = b_0 + b_1 \ln\left(\frac{k}{k_*}\right) + \frac{b_2}{2}\ln^2\left(\frac{k}{k_*}\right) + \cdots. \quad (34)$$

Exponentiation of Eq. (34) automatically enforces the positive definiteness of $\mathcal{P}(k)$ and allows us to directly link the first coefficients $b_n$ to the spectral indices and the runnings, because

$$b_{S1} = n_S - 1,\ b_{T1} = n_T,\ b_{S2} = \alpha_S,\ b_{T2} = \alpha_T. \quad (35)$$

The equivalent expressions to Eqs. (26)–(31) are

$$b_{S0} = -2(C+1)\epsilon_1 - C\epsilon_2 + \left(-2C + \frac{\pi^2}{2} - 7\right)\epsilon_1^2 + \left(-C^2 - 3C + \frac{7\pi^2}{12} - 7\right)\epsilon_1\epsilon_2 + \left(\frac{\pi^2}{8} - 1\right)\epsilon_2^2 + \left(-\frac{1}{2}C^2 + \frac{\pi^2}{24}\right)\epsilon_2\epsilon_3, \quad (36)$$

$$b_{S1} = -2\epsilon_1 - \epsilon_2 - 2\epsilon_1^2 - (2C+3)\epsilon_1\epsilon_2 - C\epsilon_2\epsilon_3, \quad (37)$$

$$b_{S2} = -2\epsilon_1\epsilon_2 - \epsilon_2\epsilon_3, \quad (38)$$

for the scalars, and

$$b_{T0} = -2(C+1)\epsilon_1 + \left(-2C + \frac{\pi^2}{2} - 7\right)\epsilon_1^2 + \left(-C^2 - 2C + \frac{\pi^2}{12} - 2\right)\epsilon_1\epsilon_2, \quad (39)$$

$$b_{T1} = -2\epsilon_1 - 2\epsilon_1^2 - 2(C+1)\epsilon_1\epsilon_2, \quad (40)$$

$$b_{T2} = -2\epsilon_1\epsilon_2, \quad (41)$$

for the tensors.

Finally, the ratio of amplitudes of scalars and tensors at the pivot point is

$$R = 16\epsilon_1\left[1 + C\epsilon_2 + \left(C - \frac{\pi^2}{2} + 5\right)\epsilon_1\epsilon_2 + \left(\frac{1}{2}C^2 - \frac{\pi^2}{8} + 1\right)\epsilon_2^2 + \left(\frac{1}{2}C^2 - \frac{\pi^2}{24}\right)\epsilon_2\epsilon_3\right]. \quad (42)$$

TABLE III. Slow-roll values of spectral indices, their running and the tensor-to-scalar ratio for the three models considered. All quantities are evaluated at $k = 0.01h\ \mathrm{Mpc}^{-1}$.

| Slow-roll values | $R$ | $n_S - 1$ | $n_T$ | $\alpha_S$ | $\alpha_T$ |
|---|---|---|---|---|---|
| Chaotic | 0.285 | −0.055 | −0.037 | −0.0010 | −0.0007 |
| False vacuum | 0.051 | 0.054 | −0.006 | 0.0017 | 0.0004 |
| Arctan model | 0.089 | −0.221 | −0.014 | −0.0291 | −0.0041 |

This becomes the well-known ''consistency condition of inflation'' $R = -8n_T$ at leading order, which holds for single-inflaton-field slow-roll models. The values of the ratio $R$, the spectral indices and their running, computed in the slow-roll approximation for the three models envisaged in this article, are summarized in Table III. The values of the horizon-flow parameters were obtained numerically, though an actual reconstruction may also feature a slow-roll approximation in relating those to the inflationary potential.

## V. DOES THE SHAPE OF THE FITTED SPECTRA MATTER?

In the preceding section, we have shown that the shape of the slow-roll spectra does not coincide with the shape of the fit of Sec. III. From a theoretical point of view, it is clear that the former should be used not only to predict the spectra but also to fit real data. For many choices of parameters the difference between the shapes is not significant, but there are also models where this difference can be important.

An example is given in Fig. 5, where we plot

$$\mathrm{Error}(\mathcal{P}_{sr}^{fit}) \equiv \left(\frac{\mathcal{P}_{sr}^{fit}}{\mathcal{P}_{num}} - 1\right) \times 100\%, \quad (43)$$

for the arctan model of Sec. II. In this equation, $\mathcal{P}_{sr}^{fit}$ is found by considering

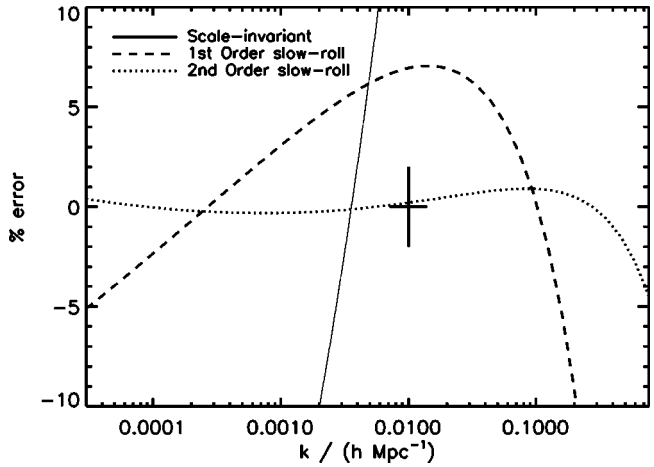


FIG. 5. Fitting the slow-roll shape to the arctan model. The errors should be compared with the errors in Fig. 3. For this model, the second-order slow-roll shape provides a better fit than the power-law plus running shape.

TABLE IV. As in Table II, but for the spectral shape that is predicted by slow-roll inflation.

| Slow-roll fit | $A_{\rm fit/num}$ | $R$ | $n_{\rm S}-1$ | $n_{\rm T}$ | $\alpha_{\rm S}$ | $\alpha_{\rm T}$ |
|---|---|---|---|---|---|---|
| Chaotic | 1.05 | 0.279 | | | | |
| | 1.01 | 0.283 | −0.056 | −0.037 | | |
| | 1.00 | 0.285 | −0.055 | −0.037 | −0.0010 | −0.007 |
| False vacuum | 0.98 | 0.053 | | | | |
| | 1.01 | 0.051 | 0.051 | −0.006 | | |
| | 1.00 | 0.051 | 0.055 | −0.006 | 0.0017 | 0.0004 |
| Arctan model | 1.23 | 0.072 | | | | |
| | 1.07 | 0.082 | −0.210 | −0.016 | | |
| | 1.00 | 0.089 | −0.213 | −0.019 | −0.0289 | −0.0044 |

$$\mathcal{P}_{\rm sr}=c_0+c_1\ln\left(\frac{k}{k_*}\right)+\frac{c_2}{2}\ln^2\left(\frac{k}{k_*}\right), \tag{44}$$

and calculating the three coefficients $c_0$, $c_1$ and $c_2$ by minimizing the quantity

$$\sum_i\,[\mathcal{P}_{\rm sr}^{\rm fit}(k_i)-\mathcal{P}_{\rm num}(k_i)]^2. \tag{45}$$

Comparing the slow-roll fit of Fig. 5 with the power-law fit of Fig. 3, we can see that the slow-roll shape does indeed provide a better fit in this case, keeping the error below 1% for most of the range. Thus the power spectrum shape can make a difference, and there exist models where fitting with the power-law instead of the slow-roll shape can lead to significant errors (defined by the criterion of Sec. III A).

However, one cannot conclude that the slow-roll shape necessarily gives a better fit in general. An example where the slow-roll fit converges slower than the power-law fit is the chaotic model, although the difference is not significant in that case. For power-law inflation the slow-roll shape will actually fare less well.

A second step is to go from the coefficients $c_0$, $c_1$ and $c_2$ to the characteristic parameters of the primordial spectra. This can be done by means of the relations

$$(n_{\rm S}-1)^{\rm fit}_{\rm sr}=\frac{c_1}{c_0}+\mathcal{O}(\epsilon_n^3), \tag{46}$$

$$(\alpha_{\rm S})^{\rm fit}_{\rm sr}=\frac{c_2}{c_0}-\frac{c_1^2}{c_0^2}+\mathcal{O}(\epsilon_n^3), \tag{47}$$

and analogous equations for the tensors. The coefficient $R$ can be obtained as

$$R^{\rm fit}_{\rm sr}=\frac{c_{0\rm T}}{c_{0\rm S}}. \tag{48}$$

The results are summarized in Table IV. This table should be compared with Tables I and II. Fitting a different shape has now the effect that the parameters of the arctan model converge, in contrast to the power-law fit.

Fitting the coefficients $c_n$ allows us to test the consistency relation of inflation, and thereafter constraining $c_{1\rm T}$ and $c_{2\rm T}$ according to Eqs. (30) and (31) allows us to measure the inflationary parameters.

Having shown that there exist situations where the shape matters, we wish to find the region of the parameter space in which the difference between a power-law shape with running and the shape predicted by slow-roll inflation is significant. For this purpose, we define the estimator

$$\sigma\equiv\frac{\mathcal{P}_{\rm sr}-\mathcal{P}_{\rm fit}}{(\mathcal{P}_{\rm sr}+\mathcal{P}_{\rm fit})/2}\times 100\% \tag{49}$$

$$\simeq-\frac{n}{2}\left(\alpha+\frac{n^2}{3}\right)\ln^3\left(\frac{k}{k_*}\right)\times 100\%, \tag{50}$$

where $n$ stands in for $n_{\rm S}-1$ or $n_{\rm T}$. Note that this estimator presumes that the two fits generate the same values for the amplitude, spectral index and running, whereas in practice a different choice of shape will lead to different values. This estimator therefore underestimates the differences between the two fits close to the pivot point and overestimates them far away from the pivot.

In Fig. 6 we plot the contours of the maximum of $|\sigma(k)|$ in the interval $-1.5<\log_{10}(k/k_*)<1.5$ in the $(n_{\rm S}-1,\alpha_{\rm S})$

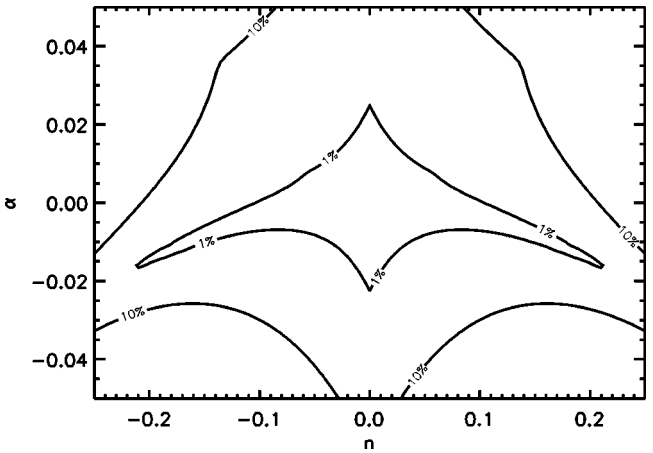


FIG. 6. The region of fitted spectral indices and runnings in which the difference between the power-law shape and the slow-roll shape, estimated by $|\sigma|$, is within 1% and within 10%.

plane. Its shape can be understood most easily from the approximation Eq. (50). We conclude that within the ranges $n_S - 1 \in [-0.05, 0.05]$ and $\alpha_S \in [-0.015, 0.015]$, shape should not matter even at the accuracy level of Planck. For present CMB experiments this plot suggests that as long as $|n_S - 1|$ is within the range shown in Fig. 6 shape is not an issue if the running is at most of order 0.01, which is the case for a wide class of inflationary models (similar constraints should be assumed to hold true for higher corrections as well).

A significant difference between the two fits at a given observational accuracy is a clear indicator that higher-order terms may be important, as it is those which give the difference between the two expansions. To be certain of robust results, an attempt should be made to estimate these higher-order terms, either by extending one or both expansions to seek convergence between them or by resorting to fully numerical analysis techniques.

## VI. ACCURACY OF SLOW-ROLL ANALYTIC SPECTRA

In the previous section we showed that spectral shape can matter and therefore that it is important to take the predictions of slow-roll inflation into account if we are interested in the physics of inflation itself. Before discussing how to extract the inflationary parameters we study the accuracy of the slow-roll approximation at second order. First studies of the accuracy of the slow-roll expansion can be found for the amplitudes in Ref. [4] by comparing to numerical results, while in Ref. [20] the first-order expressions for the amplitudes and the spectral indices has been tested by comparison to analytical results for power-law inflation. Here we extend these studies to the full power spectrum at second order. We define the error of the slow-roll power spectrum as

$$\mathrm{Error}(\mathcal{P}) \equiv \left( \frac{\mathcal{P}_{\mathrm{sr}}}{\mathcal{P}_{\mathrm{num}}} - 1 \right) \times 100\%, \tag{51}$$

where $\mathcal{P}_{\mathrm{sr}}$ is given by Eqs. (23) and (26)–(31). In these expressions the values of $H$, $\epsilon_1$, $\epsilon_2$ and $\epsilon_3$ are computed numerically for the three models of Sec. II.

Looking at the chaotic inflation model first, we can see from Fig. 7 that the error curves resulting from slow-roll predictions generally have the property that they are most accurate close to the pivot point (in terms of amplitude and spectral index) and that the error increases as we move away from the pivot point. We can also see that the second-order expressions can improve the accuracy of both the scalar and tensor power spectra to within Planck requirements, whereas the accuracy of the corresponding first-order expression would be at best marginal. This improvement is mostly brought about by the inclusion of the running.

The tensor spectrum of Fig. 7 is determined more accurately than the scalars. We have observed that this is typically the case. Since the accuracy requirement upon the tensors is less than on the scalars, it is the scalars upon which attention should be focused.

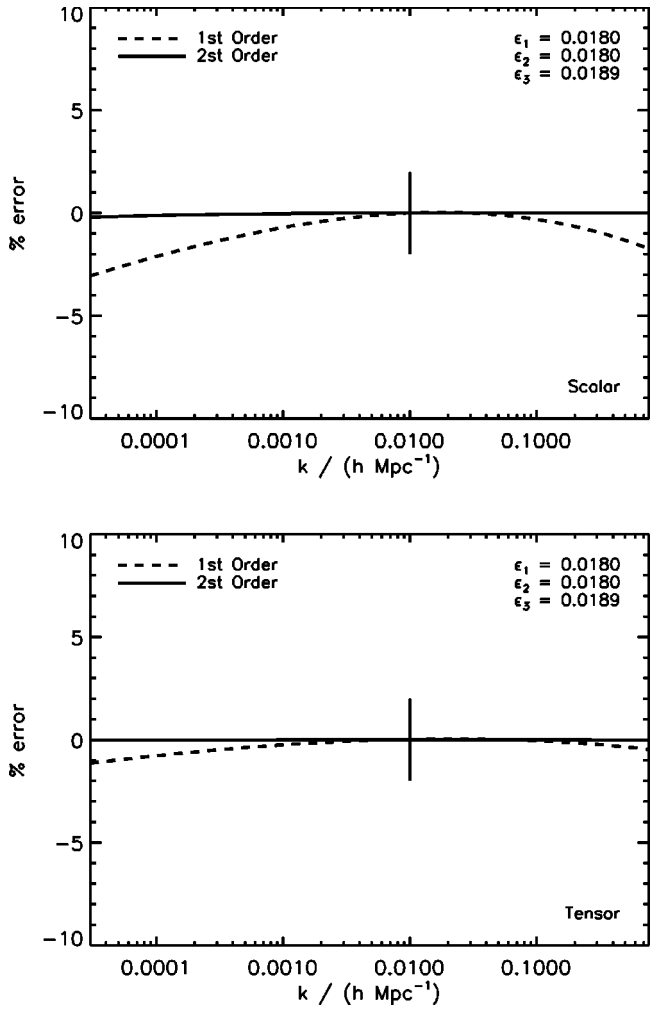


FIG. 7. Scalar and tensor error curves for the chaotic inflation potential. The pivot scale crosses the Hubble horizon 55 *e*-folds before the end of inflation. We see an improvement in accuracy from the first to the second-order expressions. The tensors have better overall accuracy than the scalars.

Next we turn to the false vacuum inflation model. Note immediately from Fig. 8 that the second-order expression improves both the shape of the power spectrum and the accuracy of the amplitude at the pivot point itself. The first-order expression is good enough for present experiments in this example, but not for MAP and Planck.

Finally, for the arctan model we see in Fig. 9 that although $\epsilon_1$ is small and $\epsilon_2$ and $\epsilon_3$ are still in agreement with the slow-roll conditions, the effect of the second-order correction is very important. The first-order expression is not sufficient for MAP. In this example, the first-order expression also produces a significant error in the amplitude at the pivot point. For Planck the plot suggests that the third order is necessary.

It is of course impossible to study the accuracy of all possible models of inflation in this way. We therefore need a more general estimator for the accuracy of the slow-roll expansion in the parameter space $\epsilon_n$. The difference between the slow-roll expansions of $\mathcal{P}(k)$ and $\ln \mathcal{P}(k)$ is such an estimator. We define the error at a given order $n$ to be

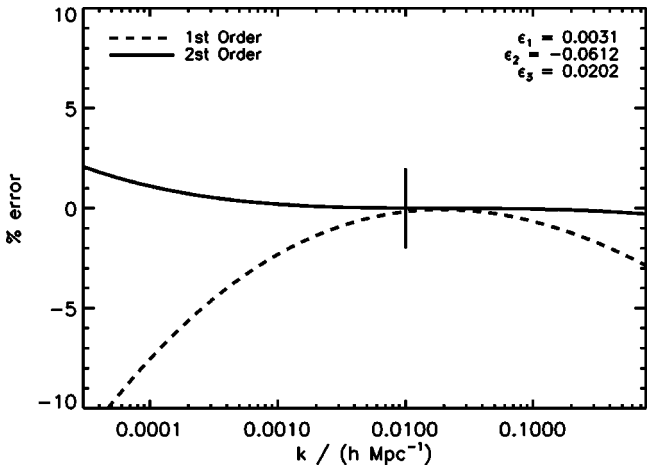


FIG. 8. Scalar error curve for the false vacuum inflation model. Again, we see an improvement in accuracy from the first to second-order expressions which helps to correct the amplitude at the pivot point.

$$\sigma_{\rm n}=\frac{\left|\sum_{i=0}^{n}\frac{a_i}{i!}\ln^i\left(\frac{k}{k_*}\right)-\exp\left[\sum_{i=0}^{n}\frac{b_i}{i!}\ln^i\left(\frac{k}{k_*}\right)\right]\right|}{\sum_{i=0}^{n}\frac{a_i}{i!}\ln^i\left(\frac{k}{k_*}\right)+\exp\left[\sum_{i=0}^{n}\frac{b_i}{i!}\ln^i\left(\frac{k}{k_*}\right)\right]}100\%, \quad (52)$$

where the coefficients $a_i$ and $b_i$ are taken at order $\epsilon_m^n$. The interpretation of this expression is that it gives the smallest fractional amount by which the worse of the two expansions departs from the true power spectrum, namely half the distance between the two estimates. This interpretation justifies the absence of a factor 1/2 at the denominator in Eq. (52).

This expression is of order $\epsilon_m^{n+1}$ and therefore is an indicator of the importance of orders that have not been included. Moreover it has the same typical behavior of the errors as one goes away from the pivot point, and we also find that it estimates the orders of the errors for the examples of Sec. II correctly. We expect that this estimate typically works well although there exists the possibility of fine-tuning models such that $\sigma_n$ is not a good estimator. In the following we study the maximum of the error in a suitable interval of wavenumbers, because a large error in a small range may spoil an otherwise accurate fit. We therefore maximize $\sigma_1(k,\epsilon_1,\epsilon_2)$ and $\sigma_2(k,\epsilon_1,\epsilon_2,\epsilon_3)$ over $-1.5<\log_{10}(k/k_*)<1.5$. This is certainly conservative but is a good indicator of when robust results are expected.

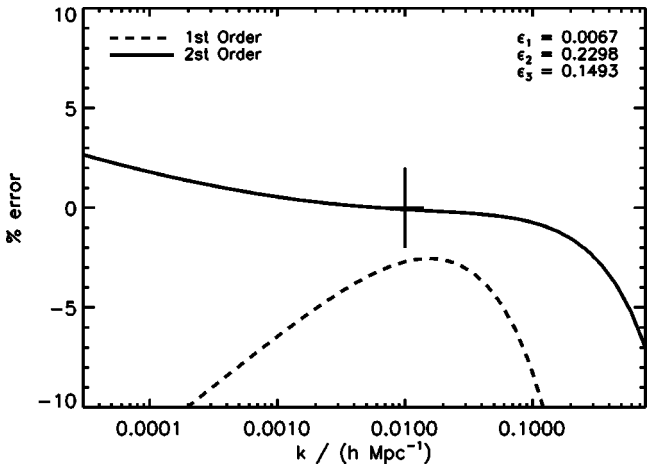


FIG. 9. Scalar error curve for the arctan potential. We see an improvement from the first to second order as well as a significant correction to the overall amplitude at the pivot scale.

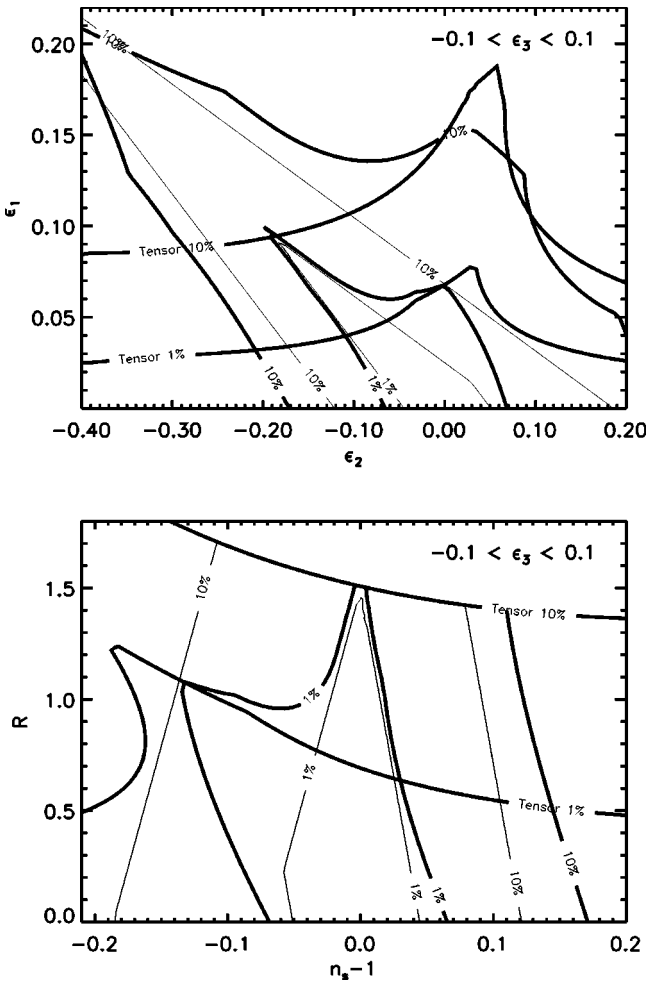


FIG. 10. These panels show the error estimate $\sigma_1$ for the slow-roll expansions at first order (thin lines) and $\sigma_2$ at second order (thick lines). The upper panel is a function of horizon-flow parameters, while the lower panel transforms this into the $(n_{\rm S}-1)-R$ plane.

The upper panel of Fig. 10 shows the error in the $\epsilon_1-\epsilon_2$ plane, maximizing over $-0.1<\epsilon_3<0.1$ (the arctan model actually lies outside this range). The scalar error contours are elongated along the direction $\epsilon_1=-\epsilon_2/2$, which corresponds to $n_{\rm S}=1$ at first order. In the top left corner $\sigma_1$ becomes independent of the dominant contribution proportional to $\ln k$ for $n_{\rm S}=1$. For $\sigma_2$ there is a similar cancellation of the $\ln^2 k$ contribution for models close to $n_{\rm S}=1$, which explains the shape of the contours. These elongated shapes are therefore a feature of our estimator $\sigma_n$; they do not reflect a proper estimate of the error in the top left corner as other higher-order terms not considered would spoil these cancellations. With the exception of that top region, we see

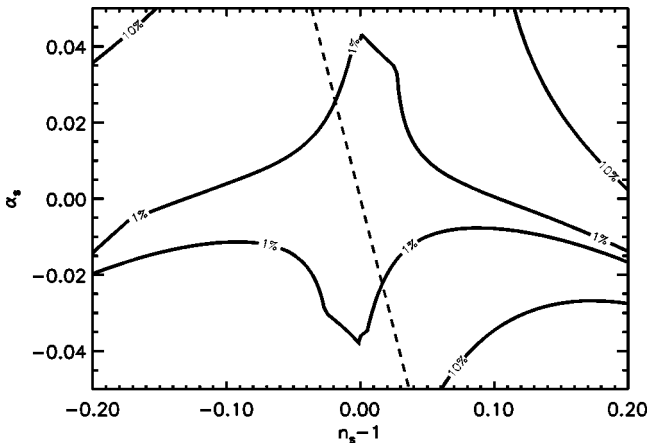


FIG. 11. The error estimate $\sigma_2$ in the $(n_S-1)-\alpha_S$ plane, with $\epsilon_1 \ll 0.001$. The dashed line is $\alpha_S=(n_S-1)/C$, in the vicinity of which the error estimate can be misleading.

that, as expected, the second-order expressions extend the area of parameter space meeting a specified accuracy requirement.

It is useful to examine these results in the $(n_S-1)-R$ plane via the transformation

$$n_S-1=-2\epsilon_1-\epsilon_2, \tag{53}$$

$$R=16\epsilon_1 \tag{54}$$

shown in the lower panel of Fig. 10. We use the first-order relations also for the second-order error contours here; the error made by this can be neglected for the present purpose. The restriction that we put on $\epsilon_3$ gives rise to values for running in the range $\alpha_S \in [-0.023,0.14]$ for the displayed region of parameter space. The first-order expression gives errors within 10% in the region given approximately by $-0.15<n_S-1<0.1$ and $R<1.5$. The second-order slow-roll expression gives an accuracy better than 1% in a somewhat smaller range of parameter space ($-0.1<n_S-1<0.05$, $R<1.0$).

It is important to stress that these regions are very conservative as we maximize the error over both $\epsilon_3$ and wave number. The conclusions of small errors in parameter space regions is therefore very robust, and indeed the errors are likely to be within acceptable levels even for many models lying outside our contours.

An important limit is when $\epsilon_1$ is very small, since a broad class of inflation models belong to this category, e.g. false vacuum dominated inflation gives rise to tiny $\epsilon_1$. When $\epsilon_1 \lesssim 0.001$, then the tensor spectrum will have no effect on the low-$l$ portion of the $C_l$ curves at the 1% level, see Eq. (42). At this point the tensor $C_l$'s drop out of reach and we can no longer measure $H$ during inflation and $\epsilon_1$ separately, see Eq. (24). The scalar power spectrum, Eqs. (26)–(28), now reduces to a function of $\mathcal{P}_{\mathcal{R}0}(k_*)$, $\epsilon_2$ and $\epsilon_2\epsilon_3$, where the last two parameters determine $n_S-1=-\epsilon_2-C\epsilon_2\epsilon_3$ and $\alpha_S=-\epsilon_2\epsilon_3$. In Fig. 11 we plot the error of the second-order power spectrum, $\sigma_2$, in the $(n_S-1)-\alpha_S$ plane. The transformation between the $(n_S-1)-\alpha_S$ plane and the $\epsilon_2-\epsilon_3$ plane

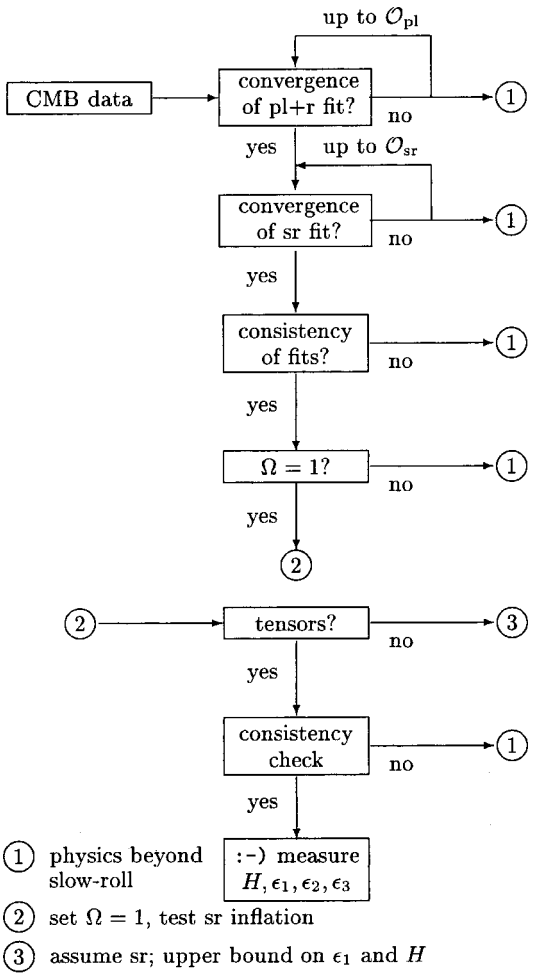


FIG. 12. Suggested pipeline to test slow-roll inflation and estimate its parameters.

is nonlinear and singular at $\epsilon_2=0$ for any $\epsilon_3$. All corresponding models have $n_S-1=\alpha_S=0$. Moreover, in the vicinity of the line $\alpha_S=(n_S-1)/C$ the value of $\epsilon_2$ becomes arbitrarily small, and thus $\epsilon_3$ can be huge. Therefore, in the vicinity of the dashed line the estimator $\sigma_2$ is misleading, because it gives a small error even for models which violate the slow-roll condition $\epsilon_3 \ll 1$. Nevertheless, the conclusion is that fairly weak running $<0.02$ can be accurately (1%) described by a slow-roll expansion with tiny $\epsilon_1$.

## VII. TESTING SLOW-ROLL INFLATION

We end with a proposal of how to proceed with testing slow-roll single-field inflation using future high-accuracy data. The corresponding data analysis pipeline is sketched in Fig. 12. The inputs are the CMB data and a cosmological model (e.g., $\Lambda$CDM). The first step should be to determine the cosmological parameters under the assumption that the power spectra of scalar and tensor perturbations are given by a power-law with running of the spectral index, see Eq. (10). One should check the convergence of the values of all cosmological parameters as one fits scale-invariant, power-law, and power-law with running spectra, as discussed in Sec. III. One should continue to refine the power spectrum shape

(adding in running of running, etc.) until the new power spectrum parameter is found to be consistent with zero. At this point one has the choice to neglect this final parameter, and this seems a sensible option. We call the order of this truncated power spectrum $\mathcal{O}_{\rm pl}$. In a similar manner one should also check the convergence of the cosmological parameter estimates while fitting to the data using scale-invariant, first-order and then second-order slow-roll shapes, up to order $\mathcal{O}_{\rm sr}$.

One should find $|\mathcal{O}_{\rm pl}-\mathcal{O}_{\rm sr}|\leqslant 1$, with $\mathcal{O}_{\rm pl}=\mathcal{O}_{\rm sr}$ being the most likely case. If we also find consistent estimates of the cosmological parameters then clearly the choice of power spectrum shape does not matter. If $\mathcal{O}_{\rm pl}\neq\mathcal{O}_{\rm sr}$ but the cosmological parameter estimates are convergent and consistent with each other, then we have some evidence that a particular power spectrum shape may be preferred. Figure 6 might be used to check whether the extracted spectral indices and runnings are expected to give rise to a significant difference between the two fits.

If there is no convergence using one or both of the power spectrum shapes, or if the different power spectrum shapes lead to significantly different estimates of the cosmological parameters, then there is either a significant problem in the assumed cosmological model or the shape of the spectrum is completely different from a power law, e.g. a pronounced bump or a step at a privileged scale [29]. Presuming the latter, within the context of single-field inflation, the optimal strategy is a direct estimation of the inflationary potential from the data itself, without using intermediate approximations such as the slow-roll expansion, as described by Grivell and Liddle [30].[5] Such a calculation must simultaneously fit all parameters, and so will also test whether the results are consistent with a flat universe; the simplest models of inflation predict $\Omega_{\rm total}=1\pm 10^{-5}$, though realistic experiments will be orders of magnitude larger in uncertainty. If so the data are consistent with inflation, but single-field slow-roll inflation would be ruled out.

If satisfactory convergence of the cosmological parameters is achieved then the next step is to check whether $\Omega_{\rm total}$ is consistent with one. If this test is failed then slow-roll inflation is excluded and we need alternative physics. If the Universe is consistent with flatness, slow-roll inflation can now be taken very seriously. In the previous section we have shown that the power of fluctuations can be predicted at the required level of accuracy in a large region of parameter space favored by present CMB observations. Once slow-roll inflation has been adopted as a working hypothesis, $\Omega_{\rm total}$ should be fixed at unity and not varied in any parameter fits.

[5]The inflationary potential is parametrized, for example by a Taylor series, and the scalar and tensor power spectra are obtained by solving the mode equations and fed into a Boltzmann code such as CMBFAST [18] or CAMB [14]. The only approximation is the validity of linear perturbation theory. The result is an unbiased estimation of the inflationary potential with automatic generation of the error covariances of the potential parameters amongst themselves and with the cosmological parameters [30]. Other considerations of single-field inflation beyond slow roll are given in Refs. [24,31].

We can now test the consistency relation and then estimate the inflationary parameters. In principle one could use either expansion [Eq. (10) or Eq. (44)] if it has been successful, and even if $\mathcal{O}_{\rm pl}\neq\mathcal{O}_{\rm sr}$ the inflationary information contained within them should be equivalent. However presuming it is available it makes best theoretical sense to use the slow-roll fit. The approach is sketched in the lower tree of the pipeline in Fig. 12.

The first step is to check whether a tensor contribution can be detected at a significant level. If not, then there are no means to fully check the specific predictions of slow-roll inflation. However, this means that an upper bound on the tensor-to-scalar ratio $R$ is provided by the CMB data. Assuming slow-roll inflation we can use the consistency relation Eq. (42) [or its first-order version Eq. (54)] to obtain an upper bound on $\epsilon_1$. Then we neglect all $\epsilon_1$ terms in Eqs. (26)–(31), allowing an estimate of $\epsilon_2$, $\epsilon_3$ and the normalization of the scalar power spectrum $H^2/\pi\epsilon_1 m_{\rm pl}^2$. Together with the upper bound on $\epsilon_1$ this gives an upper bound on the scale of inflation $H$. Figure 11 might be used to estimate the theoretical error in the measurement of $\epsilon_2$ and $\epsilon_3$. If the estimates for $|\epsilon_2|$ and $|\epsilon_3|$ turn out to be larger than the upper bound on $\epsilon_1$ we can take these estimates seriously. However, if it turns out that one of the higher-order parameters is of the same order as the upper bound for $\epsilon_1$ we cannot consistently neglect $\epsilon_1$. In this case only a banana-shaped region in parameter space of the second-order slow-roll expansion can be identified. But a warning is required at that point; without a detection of tensors it might be impossible to distinguish between single-field slow-roll inflation and other models.

If there is a significant detection of tensors, the next step is to test the consistency equation of slow-roll inflation Eq. (42). If this test is not passed, we have ruled out single-field slow-roll inflation. If we find consistency, the final step is to measure the scale of inflation $H$ and the inflationary parameters $\epsilon_1$, $\epsilon_2$ and $\epsilon_3$. By fitting directly for these parameters, rather than the coefficients of expansion as above, we are now automatically imposing the consistency relations between the scalar and tensor spectra. This is also important for measurement of the cosmological parameters, as it ensures that the uncertainties are not overestimated (under the presumption that slow-roll inflation is correct). The slow-roll shape is the preferred option for carrying out this final parameter determination, and this is also the determination which yields the definitive measures of the various cosmological parameters. These might differ from the parameters estimated from the power-law plus running fit once the consistency conditions are imposed. In particular the uncertainties should tighten as the inflationary predictions are more specific than fitting free power-laws plus running. The systematic uncertainty from theory in the measurement of inflationary parameters can now be estimated with the help of Fig. 10.

Having analytically reconstructed an inflationary potential, its validity can be checked by evaluating the perturbations generated by the potential numerically, which will provide a further estimate of the magnitude of higher-order corrections. If these prove significant, the numerical results could be used to ''tune'' the reconstructed potential with the

aim of removing any biases in the estimation of other parameters. Ultimately, analytic results obtained the way we describe can be compared with a direct numerical reconstruction as described in Ref. [30], with the two methods providing invaluable cross-checks on each other.

We have presented a strategy to measure the most important quantity in the context of inflationary models, the scale of inflation $H$. It probes the time scale and thus the energy scale of new physics, which requires the detection of tensor contributions. Sensitivity to gravitational waves is mainly provided via high-sensitivity polarization measurements, and it is these which may allow us to probe the highest energy scales for the first time.

## ACKNOWLEDGMENTS

We thank Lloyd Knox, Max Tegmark and César Terrero-Escalante for useful discussions. S.M.L. was supported by PPARC and A.R.L. in part by the Leverhulme Trust. D.J.S. acknowledges a visit to the Sussex Astronomy Centre funded by the Austrian Academy of Sciences, the Royal Society and PPARC.

[1] N.W. Halverson *et al.*, astro-ph/0104489; C. Pryke *et al.*, Astrophys. J. **568**, 46 (2002); C.B. Netterfield *et al.*, astro-ph/0104460; A.T. Lee *et al.*, Astrophys. J. Lett. **561**, L1 (2001); R. Stompor *et al.*, *ibid.* **561**, L7 (2001).

[2] J. M. Bardeen, in *Particle Physics and Cosmology*, edited by A. Zee (Gordon & Breach, New York, 1989).

[3] L.P. Grishchuk, Zh. Éksp. Teor. Fiz. **67**, 835 (1974) [Sov. Phys. JETP **40**, 409 (1974)]; V.F. Mukhanov, Pis'ma Zh. Éksp. Teor. Fiz. **41**, 402 (1985) [JETP Lett. **41**, 493 (1985)]; Zh. Éksp. Teor. Fiz. **84**, 1 (1988) [Sov. Phys. JETP **67**, 1297 (1988)]; V.F. Mukhanov, H.A. Feldman, and R.H. Brandenberger, Phys. Rep. **215**, 203 (1992).

[4] I.J. Grivell and A.R. Liddle, Phys. Rev. D **54**, 7191 (1996).

[5] L.A. Kofman and A.A. Starobinsky, Sov. Astron. Lett. **11**, 271 (1985); K.M. Górski, J. Silk, and N. Vittorio, Phys. Rev. Lett. **68**, 733 (1992); L. Knox, Phys. Rev. D **52**, 4307 (1995).

[6] J. Martin, A. Riazuelo, and D.J. Schwarz, Astrophys. J. Lett. **543**, L99 (2000).

[7] X. Wang, M. Tegmark, and M. Zaldarriaga, Phys. Rev. D **65**, 123001 (2002).

[8] J.M. Bardeen, Phys. Rev. D **22**, 1882 (1980).

[9] J. Martin and D.J. Schwarz, Phys. Rev. D **57**, 3302 (1998).

[10] D. Wands, K.A. Malik, D.H. Lyth, and A.R. Liddle, Phys. Rev. D **62**, 043527 (2000).

[11] A.D. Linde, Phys. Lett. **129B**, 177 (1983).

[12] A.D. Linde, Phys. Lett. B **249**, 18 (1990).

[13] L. Wang, V.F. Mukhanov, and P.J. Steinhardt, Phys. Lett. B **414**, 18 (1997).

[14] A. Lewis, A. Challinor, and A. Lasenby, Astrophys. J. **538**, 473 (2000).

[15] S. Hannestad, S.H. Hansen, F.L. Villante, and A.J.S. Hamilton, Astropart. Phys. **17**, 375 (2002).

[16] G. Efstathiou *et al.*, astro-ph/0109152.

[17] M. Tegmark and G. Efstathiou, Mon. Not. R. Astron. Soc. **281**, 1297 (1996).

[18] U. Seljak and M. Zaldarriaga, Astrophys. J. **469**, 1 (1996).

[19] W. Hu, Ph.D. thesis, University of California at Berkeley, astro-ph/9508126.

[20] J. Martin and D.J. Schwarz, Phys. Rev. D **62**, 103520 (2000).

[21] E.J. Copeland, I.J. Grivell, and A.R. Liddle, Mon. Not. R. Astron. Soc. **298**, 1233 (1998).

[22] E.D. Stewart and J.O. Gong, Phys. Lett. B **510**, 1 (2001).

[23] S. Dodelson and E.D. Stewart, Phys. Rev. D **65**, 101301(R) (2002); E.D. Stewart, *ibid.* **65**, 103508 (2002).

[24] D.J. Schwarz, C.A. Terrero-Escalante, and A.A. García, Phys. Lett. B **517**, 243 (2001).

[25] A.R. Liddle, P. Parsons, and J.D. Barrow, Phys. Rev. D **50**, 7222 (1994).

[26] J.E. Lidsey, A.R. Liddle, E.W. Kolb, E.J. Copeland, T. Barreiro, and M. Abney, Rev. Mod. Phys. **69**, 373 (1997).

[27] E.D. Stewart and D.H. Lyth, Phys. Lett. B, **302**, 171 (1993).

[28] A. R. Liddle and D. H. Lyth, *Cosmological Inflation and Large-Scale Structure* (Cambridge University Press, Cambridge, England, 2000).

[29] L.A. Kofman and A.D. Linde, Nucl. Phys. **B282**, 555 (1987); A.A. Starobinsky, JETP Lett. **55**, 489 (1992); J. Adams, G. Ross, and S. Sarkar, Nucl. Phys. **B503**, 405 (1997).

[30] I.J. Grivell and A.R. Liddle, Phys. Rev. D **61**, 081301(R) (2000).

[31] W.H. Kinney, Phys. Rev. D **56**, 2002 (1997); T. Souradeep, J.R. Bond, L. Knox, G. Efstathiou, and M.S. Turner, astro-ph/9802262.